energies

MDPI

Article

Optimization of Low-Power Line-Start PM Motor Using Gray Wolf Metaheuristic Algorithm

Łukasz Knypiński [1,*], Karol Pawełoszek [1] and Yvonnick Le Menach [2]

[1] Institute of Electrical Engineering and Electronics, Poznan University of Technology, Piotrowo 3A, 60-965 Poznań, Poland; karol.paweloszek@student.put.poznan.pl

[2] Laboratory of Electrical Engineering and Power Electronics (L2EP), University of Lille, Bât. ESPRIT, 59655 Villeneuve d'Ascq, France; yvonnick.le-menach@univ-lille.fr

* Correspondence: lukasz.knypinski@put.poznan.pl; Tel.: +48-61-665-2636

Received: 11 February 2020; Accepted: 3 March 2020; Published: 5 March 2020

Abstract: The paper presents the optimization method and computer software for the design of a low-power line-start permanent magnet synchronous motor (LSPMSM). The in-house-developed computer software was created with two independent modules: (a) the optimization procedure and (b) the numerical model of the motor. The optimization procedure used was a metaheuristic optimization method based on the gray wolf algorithm. Four design variables linked to the rotor structure were selected. The optimization process was performed from the rotor of a low-power induction motor (IM). The prototype of the motor (LSPMSM) was then built. The experimental measurements were performed for base the IM and optimized LSPMSM. The results of the measurements were compared for both motors. The experimental results confirmed the better performance of the designed motor in comparison to the induction motor.

Keywords: line-start permanent magnet synchronous motor; optimal design; metaheuritsic algorithm; gray wolf optimization method; efficiency

1. Introduction

In the last two decades of the 20th century, magnetic materials based on rare earth materials with a high energy density were introduced into production on a massive scale. Materials of this type are characterized by better magnetic, mechanical and thermal properties in comparison with the types of hard magnetic previously materials used in the construction of electric machines. Therefore, a dynamic development in new permanent magnet machine designs has been observed for several years. In contemporary drive systems, electric machines such as synchronous motors (PMSM), brushless DC motors and hybrid stepper motors are used increasingly often [1–3]. Currently, even motors with power given in megawatts are manufactured [4]. The development of permanent magnet motors goes hand in hand with the development of the power supply converter and advanced control algorithms.

PMSM must be powered by the inverter system, which increases the total cost of the propulsion system. In recent years, an interesting alternative for PMSM has been permanent magnet (PM) motors with self-starting ability, so-called line-start permanent magnet motors. The basic advantage of the LSPMSM is the possibility of direct start-up after connecting to a three-phase grid. Figure 1 presents the new design of different PM motors [5–7].

As new hard and soft magnetic materials are developed, innovative synchronous machine designs with permanent magnets are beginning to appear [8]. Their aim is to improve the functional parameters, characteristics and economic indicators, i.e., to reduce production and operational costs. The new designs are often more difficult to construct technologically [5]. Therefore, powder technology, which

consists of manufacturing soft magnetic materials and forming permanent magnets, is used very often [9].

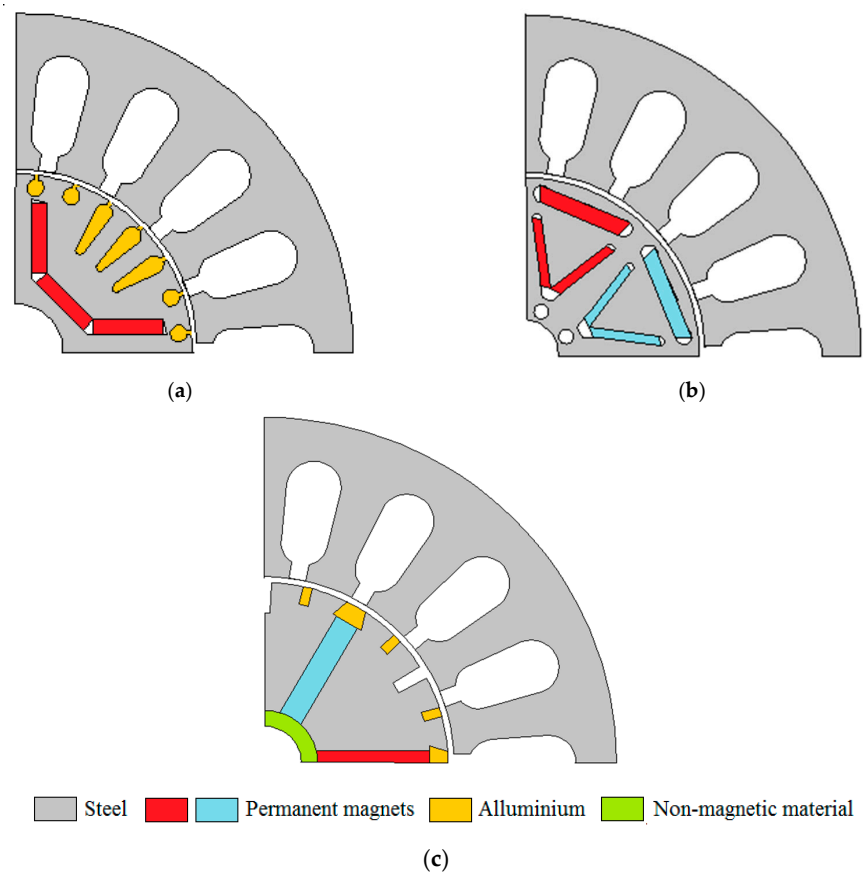

Figure 1. The modern structures of PM motors: (**a**) LSPMSM; (**b**) PMSM with delta shape magnets; (**c**) LSPMSM with composite solid rotor.

The further development of new designs of permanent magnet motors depends on the improvement of methods of simulating their operating conditions as well as methods of design and optimization. In the contemporary process of designing of electromechanical devices and systems, computer simulations are used [10]. The FEA (Finite Element Analysis) method is very popular and commonly used in the design and optimization process [6,11,12]. It allows the costly and time-consuming stage of construction of prototypes to be avoided. Simulation tools provide the designer with the possibility of a virtual "implementation" and verification of their ideas, already at the design stage, which significantly shortens the period of implementation of new projects. The costs of producing subsequent prototypes of the designed machine are also reduced.

In the last decade, non-deterministic algorithms based on observations of the natural environment (nature-inspired algorithm [13]) have been intensively developed. Scientists are still proposing new, more efficient optimization algorithms. These algorithms are based on the observation of animal behavior. This group includes: the Cuckoo Search Algorithm, the Bat Algorithm, the Particle Swarm Algorithm, the Grasshopper Optimization Algorithm and also the Gray Wolf Optimizer.

The aim of this paper was to design a low-power line-start synchronous motor. A stator for the serially manufactured low-power induction motor was used. The structural parameters of the permanent magnets and selected parameters of the rotor were optimized. In-house computer software supporting the design process of LSPMSM was developed. The software consists of two independent modules: (a) the FEA model of LSPMSM and (b) the optimization procedure. In the optimization

procedure, the gray wolf method was applied [14]. Four design variables, which describe the excitation system, have been taken into consideration.

In this paper, the optimization method and design of low-power line-start permanent magnet motor is presented. The structures of the base IM and designed LSPMSM are shown in Section 2. Then, the gray wolf optimization method is described. In Section 4, the formulation of the optimization task is discussed. Furthermore, experimental validation of the LSPMSM prototype is demonstrated in Section 5. Finally, conclusions are drawn in Section 6.

2. Structures and Parameters of the Motors

2.1. Base Induction Motor

An induction motor type SH-71-4a, available in commercial offers, was adopted to build the prototype of the LSPMSM. The rated parameters of the induction motor are presented in Table 1. The stator from the induction motor has the following parameters: outer diameter of the stator D_s = 106.4 mm, inner diameter of the stator d_s = 61.25 mm, stack length l_s = 43 mm, number of slots in the stator N_s = 24. The stator winding is wound with a single layer three-phase winding and is star-connected. The rotor cage winding has 18 bars made of aluminum.

Table 1. Rated parameters of induction motorSH-71-4a.

Parameter	Symbol	Value	Unit
Rated voltage	V_N	400	[V]
Rated power	P_N	250	[W]
Rated current	I_N	0.85	[A]
Rated velocity	n_N	1380	[rpm]
Rated torque	T_N	1.73	[Nm]
Efficiency	η	66	[%]
Power factor	cosϕ	0.64	[–]

2.2. The Designed the Low-power Line-start Permanent Magnet Synchronous Motor

In the designed LSPMSM, the stator from an induction motor without skewed slots was adopted. The rotor from the conventional induction motor was converted into a rotor with a squirrel cage and permanent magnet. The structure parameters (dimensions) of the permanent magnets were selected in such a way as to ensure functional parameters similar to or better than those of the induction motor. The rotor structure from the induction motor is presented in Figure 2a. Figure 2b shows the view of the rotor with milled gaps prepared for the mounting of permanent magnets. The complete rotor structure of the LSPMSM, consisting of the permanent magnets and cage bars, is shown in Figure 2c.

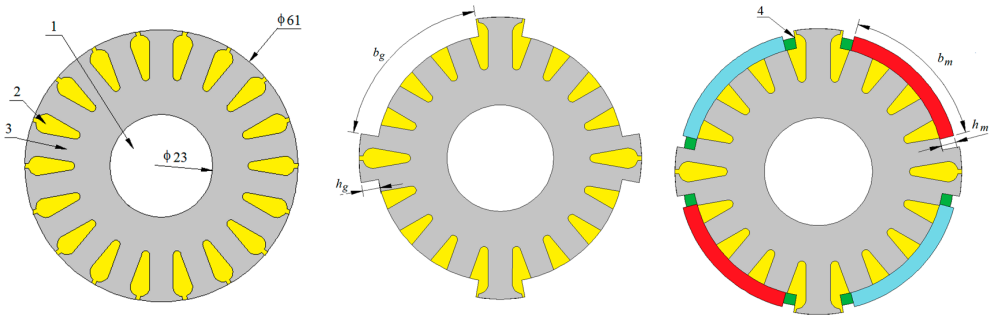

(**a**) (**b**) (**c**)

Figure 2. Structure of the rotor: (**a**) rotor from an induction motor; (**b**) rotor with milled gaps; (**c**) rotor with mounted permanent magnets (1—shaft, 2—rotor core, 3—aluminum bars, 4—non-magnetic wedge).

For the construction of the PM rotor, four pieces of permanent magnet were used. The designed motor is equipped with permanent magnets N35 H with the following properties: remanence B_r = 1.17 T and coercive force H_c = 780 kA/mat 20 °C.

3. The Gray Wolf Optimization Method

The gray wolf optimization (GWO) method was developed on the basis of hunting techniques used by wolves in 2014 [15]. The GWO method can be very effective in comparison to other non-deterministic optimization methods [16]. The optimization process is the result of an interaction between individuals, which try to look for prey together. A wolf pack usually consists of several individuals in their natural environment. The pack leader, individual α, is the best-adapted individual in the pack. In the wolf pack's organization, a very extensive system of social rungs is observed. The most important individual is the α. The alternative leader of the pack is the β individual. The third level in the hierarchy comprises δ individuals. The rest of the individuals in the algorithm are called ω individuals. These individuals represent the lowest level in the pack hierarchy. The positions of each ω individual are determined on the basis of position of the α, β and δ in each discrete time step [17]. The hunting process of a gray wolf can be divided into several stages: (a) the stage of searching for the prey, (b) the stage of the chase, (c) the stage of encircling the prey and (d) the stage of the attack [14].

In the mathematical model of the GWO method, the discrete position of each ω individual is determined in the subsequent iterations. The vector of positions of the *i*-th individual in the *k*-th iteration is calculated as follows:

$$\mathbf{X}_k^i = \frac{\mathbf{X}_1 + \mathbf{X}_2 + \mathbf{X}_3}{3} \tag{1}$$

Vectors $X_1[1, 2, \ldots, n]$, $X_2[1, 2, \ldots, n]$ and $X_3[1, 2, \ldots, n]$ in Equation (1) are closely related to the position of the α, β and δ individuals in the area of the solved optimization task, where n is the number of design variables in the optimization process. In the GWO method, the value of X_1, X_2 and X_3 can be expressed as in the formula below,

$$\mathbf{X}_1 = \mathbf{X}_{k-1}^{\alpha} - A_k^{\alpha} D^{\alpha},\ \mathbf{X}_2 = \mathbf{X}_{k-1}^{\beta} - A_k^{\beta} D^{\beta}, \mathbf{X}_3 = \mathbf{X}_{k-1}^{\delta} - A_k^{\delta} D^{\delta} \tag{2}$$

where $\mathbf{X}_{k-1}^{\alpha}$, $\mathbf{X}_{k-1}^{\beta}$ and $\mathbf{X}_{k-1}^{\delta}$ are the vectors of positions of α, β and δ in the previous iteration of the algorithm, A_k^{α}, A_k^{β} and A_k^{δ} are the random control parameters of the GWO method.

The values of variables D^{α}, D^{β} and D^{δ} in the gray wolf method represent the distance between the wolf under consideration and the leaders of the wolfpack (individuals α, β and δ) and can be determined using the formula,

$$D^{\alpha} = \left|C_1 \mathbf{X}_{k-1}^{\alpha} - \mathbf{X}_{k-1}^{i}\right|, \quad D^{\beta} = \left|C_2 \mathbf{X}_{k-1}^{\beta} - \mathbf{X}_{k-1}^{i}\right|, \quad D^{\delta} = \left|C_3 \mathbf{X}_{k-1}^{\delta} - \mathbf{X}_{k-1}^{i}\right| \tag{3}$$

where C_1, $C_2$and C_3 are the coefficient of the GWO method.

The value of coefficients C changed randomly regardless of the locations of the remaining individuals in the pack. These coefficients are determined randomly for each individual and are calculated as follows:

$$C_1 = 2r_1, \quad C_2 = 2r_2, \quad C_3 = 2r_3 \tag{4}$$

where r_1, r_2 and r_3 are the random numbers from range (0, 1).

In each iteration of the method, it is necessary to determine the actual value of parameter A. The control parameters A determine the ability of the wolves to move in the area of the task [18]. Adopting large values for A, the ω individuals are very mobile and can freely move. A low value of this parameter makes the algorithm a local search properties algorithm. In the algorithm developed below, the values of the coefficients A_k^{α} A_k^{β} and A_k^{δ} are calculated as follows:

$$A_k^{\alpha} = 2a_k r_1,\ A_k^{\beta} = 2a_k r_2,\ A_k^{\delta} = 2a_k r_3 \tag{5}$$

In the gray wolf method, the value of coefficient a is determined for each iteration. This factor usually decreases linearly [19]. In the proposed algorithm, the value of coefficient a is determined for each iteration according to formula [20].

$$a_k = 0.25 + 5e^{-k} \tag{6}$$

During successive iteration of the optimization process, the global extreme is surrounded by virtual wolves. The best positions are ensured tothe α, β and δ individuals (see Figure 3). The rest of the individuals update their position according to the reference positions for α, β and δ. The determination of the new positions of the random ω positions are shown in Figure 3.

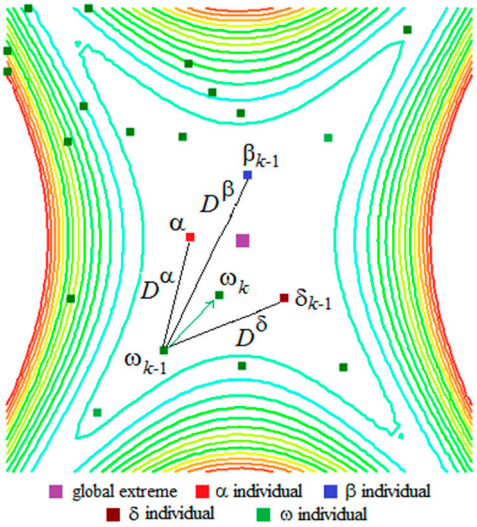

Figure 3. The determination of new position of ω individual.

4. Formulation of the Design Problem

The purpose of the optimization was to determine the dimensions (see Figure 2) of the permanent magnet (b_m and h_m), relative span (b_g) and dept of milled gaps (h_g) in the rotor, which will ensure better operational parameters of designed LSPMSM in comparison to IM. During optimization calculation only selected parameters of the rotor geometry were changed. All stator dimensions remain constant over optimization process.

Four design variables have been assumed (see Figure 2): $s_1 = \alpha_g = b_g/\tau$—the relative span of milled gap in rotor, $s_2 = \xi = h_b/h_m$—relative dept of milled gap in rotor, $s_3 = h_m$—thickness of the permanent magnet, $s_4 = \alpha_m = b_m/\tau$—relative span of the permanent magnet, where τ is the pole pitch. The design variables form the vector $s = [\alpha_g, \xi, h_m, \alpha_m]^T$. The ranges of change for all design variables are given in Table 2.

Table 2. The ranges of design variables during optimization process.

Design Variable	min Value	max Value	Unit
α_g	0.75	0.95	[–]
ξ	1.05	1.6	[–]
α_m	0.6	0.9	[–]
h_m	3.0	5.5	[mm]

Very often the normalization of design variables is performed to standardize their value in the optimization process. The purpose of the normalization is to make design variables comparable. The design variables $s_j$is converted into dimensionless quantities x_j according to the relationship

$$x_j = \frac{s_j - s_{j\min}}{s_{j\max} - s_{j\min}} \tag{7}$$

where $s_{j\min}$ and $s_{j\max}$ are the lower and upper limits of each variable s_j, respectively.

An optimum design is focused on the rotor structure construction and is aimed at improving the motor performance [21–24]. The functional parameters taken into account during the optimization process are: (a) motor efficiency, (b) power factor and (c) starting capability. In an elaborated algorithm, the optimization problem with many objectives has been transformed to a single objective function consisting of all objectives [6,25,26]. Such an approach is known from the linear programming method. The objective function for *i*-th wolf is written as,

$$f^i(\mathbf{x}) = \chi\left(\frac{\eta^i(\mathbf{x})}{\eta_0}\right)^{w_1}\left(\frac{\cos\phi^i(\mathbf{x})}{\cos\phi_0}\right)^{w_2} \tag{8}$$

where χ is the coefficient determines of the quality of synchronization capability, $\eta^i(\mathbf{x})$, $\cos\phi^i(\mathbf{x})$ are themotor efficiency and motor power factor for the *i*-th individual, w_1, w_2 are the weighting factor, η_0, $\cos\phi_0$ are the average values of efficiency and power factor obtained during the initiation procedure of the wolf pack and remaining constant during the optimization process.

In the developed algorithm for each individual, a transient simulation of the start-up of the designed machine is carried out. On the basis of this simulation, it is possible to assess the synchronization capabilities of the motor. The value of the χ coefficient is assumed as follows:

$$\chi = \begin{cases} 1 & \text{if} \quad n = n_s \\ 0.1 & \text{if} \quad n < n_s \end{cases} \tag{9}$$

where n is the steady-state rotational velocity of the motor, n_s is the synchronous rotational velocity.

The design process of the low-power line-start PM synchronous motor has been carried out using in-house developed software. The most important part of the in-house software is the optimization solver. The optimization solver has been elaborated in Delphi 7.0 environment. It contains the gray wolf optimization method and is combined with a 2D FEM model of LSPMSM. The optimization solver uses a normalized vector of design variables x. The FEM model of the motor requires the real value of design variables. Therefore, a variable transformer must be used between the optimization solver and the FEM model of LSPMSM. The block diagram of the in-house software is presented in Figure 4.

The optimization calculations have been performed for wolf pack with 38 individuals. For this number of individuals, a compromise was reached between the accuracy of finding the global extreme and the time of calculation [6]. As a stop criterion, the maximum number of optimization algorithm iteration $k_{\max}$ has been assumed. The value of a parameter is decreased according to Equation (6). The weighting coefficients of optimization procedure have been assumed as: $w_1 = 1$ and $w_2 = 1$. The value of the loading torque was equal to the rated torque T_N for the induction motor. The initial positions of all wolves in the initiation procedure were generated randomly. The results of optimization process are presented in Table 3. The value of $\eta_0 = 73.367\%$ and $\cos\phi_0 = 0.683$. In the successive columns are listed: number of iterations, design variables, phase current, efficiency, power factor and objective function. Table 3 contains the data for the α individual in the pack.

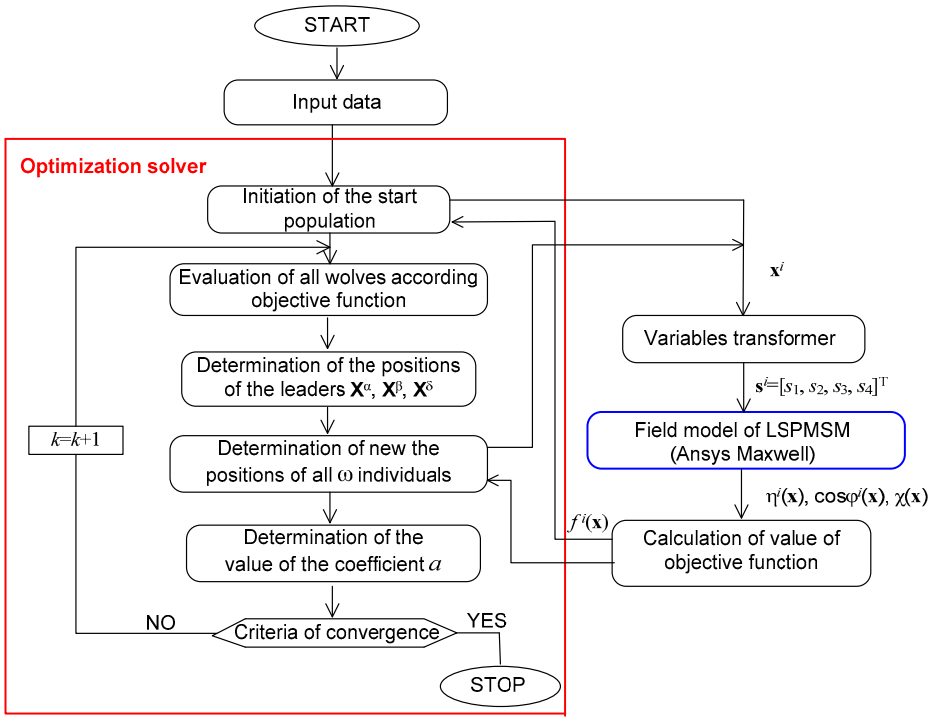

Figure 4. The flowchart of the elaborated in-house software.

Table 3. Results of optimization calculation for selected iteration of optimization procedure.

k	α_g	ξ	h_m	α_m	I_a	$\eta(\mathbf{x})$	n	$\cos\phi(\mathbf{x})$	$f(\mathbf{x})$
	[–]	[–]	[mm]	[–]	[A]	[%]	[rpm]	[–]	[–]
1	0.826	1.199	3.922	0.642	0.742	81.48	1500	0.764	1.240806
5	0.912	1.499	3.251	0.788	0.719	81.93	1500	0.835	1.363643
20	0.907	1.471	3.763	0.791	0.726	86.25	1500	0.852	1.465318
25	0.907	1.471	3.763	0.791	0.726	86.25	1500	0.852	1.465318

Based on the results of computer simulation, it can be concluded that the optimization process has been carried out correctly. The values of all functional parameters of the designed motor have significantly improved in the subsequent iterations. The power factor value was improved by about 12%. The efficiency of the motor for the best individual has been improved about by 6% in comparison to the first iteration.

5. Experimental Investigation of LSPMSM Prototype

A three-phase four-pole LSPMSM equipped with the optimized rotor has been manufactured. The stator consists of 24 slots and is equipped with three-phase single-layer overlapping winding.

The rotor cage has 18 bars made from aluminum. Four gaps were milled on the surface of the rotor. The rotor with milled gap for mounting magnets is shown in Figure 5. Four pieces of the permanent magnet were glued into milled gaps.

A photo of lab test setup for experimental verification of motor prototype is presented in Figure 6. The lab setup was adjusted to determine the functional parameters of the prototype. An experimental setup included motor prototype, eddy-current brake, power measurement system and load measurement system. The eddy-current brake consists of two discs made from (a) aluminum with a radius equal to 85 mm and (b) steel with a radius equal to 80 mm. An aluminum disc was mechanically connected with a shaft of LSPMSM. The twenty-disc permanent magnets made of N38

neodymium material were glued to steel disc surface. The load measurement system was built from (a) Arduino Nano, (b) single point mini load cell N27 and (c) SparkFun Load Cell Amplifier type HX711.

Figure 5. The manufactured rotor with milled slots.

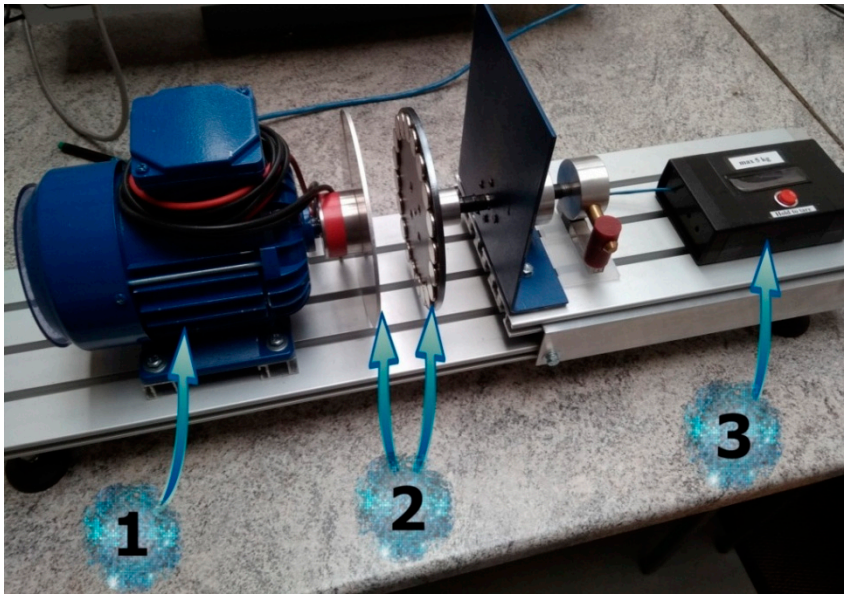

Figure 6. The lab test setup (1—LSPMSM prototype, 2—PM eddy current brake, 3—load measurement system).

Measurements of the prototype were performed in case of supplying by rated value of line voltage equal V_N = 400 V. The influence of the load torque on the motor functional parameters, as a motor efficiency power factor, as well as the phase current, was examined. The results obtained for LSPMSM were compared with the results for the induction motor. Figure 7 illustrates the comparison of efficiency and power factor and phase current for the designed LSPMSM and induction motor (IM).

It can be observed that, according to experimental results, for the low value of load torque below $0.2T_N$, the induction motor has a better cosϕ and η than LSPMSM. The LSPMSM has much better parameters for bigger values of load torque. The application of a hybrid rotor can obtain greater rated power in comparison to IM. The rated power of LSPMSM is equal to 381.5W. In LSPMSM, magnetic flux is produced by the permanent magnets in rotor. Therefore, reactive power drawn from network supply network is compensated. As shown in Figure 7a, the compensation of reactive power increases the value of the power factor. The LSPMSM has a bigger phase current in comparison to IM in a no-load condition (see Figure 7c). Increasing the efficiency and power factor in LSPMSM decreases

the value of the current drawn from the supply network with the same active power consumption. Changes in the phase current in the function of load torque depends on values of U/E, where U is the phase voltage and E_0 is back-inducted EMF. A detailed analysis of these phenomena is presented in [27].

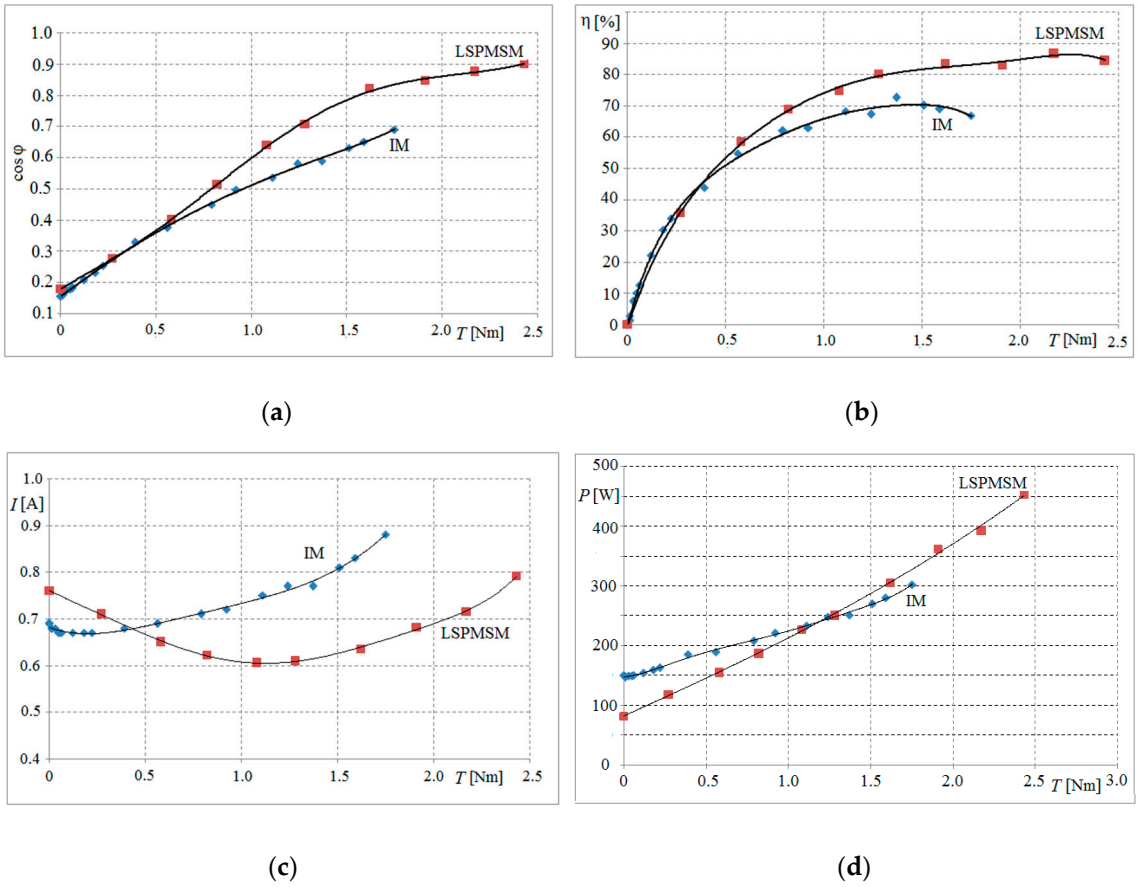

Figure 7. Comparison of functional parameters for LSPMSM and IM: (**a**) power factor; (**b**) efficiency; (**c**) phase current, (**d**) electric power.

Table 4 contains a comparison of the functional parameters in steady-state operation for the primary induction motor and line-start permanent magnet synchronous motor for constant load torque T_l equal rated torque.

Table 4. Comparison of selected parameters during laboratory test for T_l = 1.73 Nm.

Parameter	IM	LSPMSM
cosϕ[–]	0.690	0.847
η [%]	66.766	84.931
I [A]	0.861	0.682
P [W]	251.04	289.24
n [rpm]	1378	1500

Based on the presented measurement results for both motors, it can be noted that, for the rated value of load torque, a significant improvement in all functional parameters was observed. As a result of the optimization process, the power factor has improved by about 23% in comparison to the induction motor. The efficiency of the LSPMS built using a stator from induction motor has also been significantly improved. Steady-state phase current has reduced by approximately 20% in comparison to the induction motor. During correct start-up, the synchronous motor must attain the synchronous

speed [28,29]. The start-up process was performed for the supplied voltage in the range of $0.85V_N$ to V_N. In each of the tested cases, the designed LSPMSM pulls into a synchronism state.

A good correlation between measurements and simulation results was obtained. The difference between the computer simulation results and measurements was about 0.61% for the power factor of the motor. In the case of efficiency, the difference is about 1.53%.

6. Conclusions

In the article, the algorithm and computer software for the designing small-power line-start permanent magnet motors is presented. The gray wolf metaheuristic algorithm was applied in an optimization module. Using elaborated software, the computer-aided design of LSPMSM was performed. A hybrid rotor equipped in cage-winding and permanent magnet instead of the conventional cage rotor from the induction motor was designed. In the rotor, four pieces of the rotor cage were milled. Four pieces of arc-permanent magnet were glued in milled slots.

The optimization process was focused on the improvement in the functional parameters of the motor related to energy efficiency. During the optimization process, the maximized parameters were significantly improved in comparison to the classical squirrel cage induction motor. The prototype was made using optimization results. The efficiency and power factor of the designed motor were determined on the basis of measurements. A significant improvement in the functional parameters in relation to the classical induction motor was attained.

In future research, the optimization solver will be supplemented with other non-deterministic optimization methods, such as particle swarm optimization algorithm and cuckoo search algorithm. Afterwards, the authors plan to perform a comparative calculation for various optimization methods.

Author Contributions: Conceptualization, Ł.K. and Y.L.M.; methodology, Ł.K.; software, Ł.K.; validation, Ł.K. and K.P.; formal analysis, Ł.K.; investigation, K.P.; data curation, Ł.K.; writing—original draft preparation, Ł.K.; review and editing, Y.L.M. All authors have read and agreed to the published version of the manuscript.

Funding: This research was funded by the Polish Government, grant number [0212/SBAD/0484].

Conflicts of Interest: The authors declare no conflict of interest.

References

1. Zöhra, B.; Akar, M.; Eker, M. Design of novel line-start synchronous motor rotor. *Electronics* **2019**, *8*, 25. [CrossRef]
2. Praveen, R.P.; Ravichandram, M.H.; SadasivanAchari, V.T.; Jagathy, R.; Madhu, G.; Bindu, G.R. Design and finite element analysis of hybrid stepper motor for spacecraft applications. In Proceedings of the IEEE International Electric Machines and Drives Conference, Miami, FL, USA, 3–6 May 2009. [CrossRef]
3. Yoon, K.-Y.; Beak, S.-W. Robust design optimization with penalty function for electric oil pumps with BLDC motors. *Energies* **2019**, *12*, 153. [CrossRef]
4. Zawilak, J.; Gwoździewicz, M. Start-up of large power electric motors with high load torque. *PrzeglądElektrotechniczny* **2019**, *95*, 145–148. [CrossRef]
5. Yan, B.; Wang, X.; Yang, T. Comparative investigation of composite solid rotor applied to line-start permanent magnet synchronous motors. *IEEE Trans. Magn.* **2018**, *54*, 11. [CrossRef]
6. Jedryczka, C.; Knypiński, Ł.; Demenko, A.; Sykulski, J. Methodology for cage shape optimization of a permanent magnet synchronous motor under line start condition. *IEEE Trans. Magn.* **2018**, *54*, 8102304. [CrossRef]
7. Hwang, M.; Han, J.; Kim, D.; Cha, H. Design and analysis of rotor shapes for IPM motors in EV power traction platforms. *Energies* **2018**, *11*, 2601. [CrossRef]
8. Krings, A.; Boglietti, A.; Cavagnino, A.; Sprague, S. Soft Magnetic Material Status and Trends in Electric Machines. *IEEE Trans. Ind. Electron.* **2017**, *63*, 2405–2414. [CrossRef]
9. Ślusarek, B.; Kapelski, D.; Antal, L.; Zalas, P.; Gwożdziweicz, M. Synchronous motor with hybrid permanent magnets on the rotor. *Sensors* **2014**, *14*, 12425–12436. [CrossRef]

10. Barański, M. FE analysis of coupled electromagnetic-thermal phenomena in the squirrel cage motor working at high ambient temperature. *COMPEL* **2019**, *38*, 1120–1132. [CrossRef]
11. Aubertin, M.; Tounzi, A.; Le Menach, Y. Study of an electromagnetic gearbox involving two permanent magnetsynchronous machines using 3-D-FEM. *IEEE Trans. Magn.* **2008**, *44*, 4381–4384. [CrossRef]
12. Ghoroghchian, F.; Aliabad, A.D.; Amiri, E. Design improvement of dual-pole LSPM synchronous motor. *IET Electr. Power Appl.* **2019**, *13*, 742–749. [CrossRef]
13. Zang, H.; Zhang, S.; Hapeshi, K. A review of nature-inspired algorithm. *J. Bionic Eng.* **2010**, *7*, s232–s237. [CrossRef]
14. Ren, Y.; Te, T.; Huang, M.; Feng, S. Gray wolf optimization for multi-constrains second-order stochastic dominance portfolio optimization. *Algorithms* **2018**, *11*, 72. [CrossRef]
15. Mirjalili, S.; Mirjalili, S.M.; Lewis, A. Gray wolf optimizer. *Adv. Eng. Softw.* **2014**, *69*, 46–61. [CrossRef]
16. Mirjalili, S. How effective is gray wolf optimizer in training multi-layer perceptrons. *Appl. Intell.* **2015**, *43*, 150–161. [CrossRef]
17. Gao, Z.-M.; Zhao, J. An improved grey wolf optimization algorithm with variable weights. *Comput. Intell. Neurosci.* **2019**, *2019*, 1–13. [CrossRef]
18. Qais, M.; Hasanien, H.; Alghuwainem, S. Augmented grey wolf optimization for grid-connected PMSG-based wind energy conversion systems. *Appl. Soft Comput.* **2018**, *69*, 504–515. [CrossRef]
19. Arora, S.; Singh, H.; Sharma, M.; Sharma, S.; Anand, P. A new hybrid algorithm based on gray wolf optimizer and cow search algorithm for unconstrained function optimization and feature selection. *IEEE Access* **2019**, *7*, 26343–26361. [CrossRef]
20. Knypiński, Ł. Adaptation of the penalty function method to genetic algorithm in electromagnetic devices designing. *COMPEL* **2019**, *38*, 1285–1294. [CrossRef]
21. Kahourzade, S.; Mohmoudi, A.; Uddin, M.N. Design and performance improvement of a line-start PMSM. In Proceedings of the IEEE Energy Conversion Congress and Exposition, Denver, CO, USA, 15–19 September 2013; pp. 5042–5047.
22. Di Barba, P.; Mongaschi, M.E.; Najmeh, R.; Lowther, D.; Rahman, T. Many-objective shape optimization of IPM motors for electric vehicle traction. *Int. J. Appl. Electromagn. Mech.* **2019**, *60*, s149–s162. [CrossRef]
23. Sorgdrager, A.J.; Wang, R.J.; Grobler, A. Multiobjective design of a line-start PM motors using the Taguchi method. *IEEE Trans. Ind. App.* **2018**, *54*, 1461–4176. [CrossRef]
24. Berbecea, A.C.; Kreuawan, S.; Gillon, F.; Brochet, P. A parallel multiobjective optimization: The finite element met method in optimal design and model development. *IEEE Trans. Magn.* **2010**, *46*, 2868–2871. [CrossRef]
25. Li, M.; Yang, S.; Liu, X. Bi-goal evolution for many-objective optimization problems. *Artif. Intell.* **2015**, *228*, 45–65. [CrossRef]
26. Kamal, M.; Gupta, S.; Chatterjee, P.; Pamucar, D.; Stevic, D. Bi-Level multi-objective production planning problem with multi-choice parameters: A fuzzy goal programming algorithm. *Algorithms* **2019**, *12*, 143. [CrossRef]
27. Qui, H.; Zhang, Y.; Hu, K.; Yang, C.; Yi, R. The influence of stator winding turns on the steady-state performances of line-start permanent magnet synchronous motor. *Energies* **2019**, *12*, 2363. [CrossRef]
28. Wymeersch, B.; Belie, F.; Rasmussen, C.; Vandevelde, L. Classification method to define synchronization capability limits of line—Start permanent magnet motor using mesh-based magnetic equivalent circuit computation results. *Energies* **2018**, *11*, 998. [CrossRef]
29. Rabbi, S.; Rahman, M.A. Critical criteria for successful synchronization of line-start IPM motor. *IEEE J. Emerg. Sel. Top. Power Electron.* **2014**, *2*, 348–358. [CrossRef]